The recent development on MgH system by 16 wt% nickel addition and particle size reduction through ball milling: A noticeable hydrogen capacity up to 5 wt% at low temperature and pressure

by Ismail Ismail

Submission date: 03-Nov-2020 10:00AM (UTC+0700)
Submission ID: 1434567715
File name: development_on_MgH_International_Journal_of_Hidrogen_Energy.pdf (2.37M)
Word count: 7947
Character count: 40456

INTERNATIONAL JOURNAL OF HYDROGEN ENERGY 45 (2020) 29046–29058

Available online at www.sciencedirect.com

ScienceDirect

journal homepage: www.elsevier.com/locate/he

The recent development on MgH_2 system by 16 wt% nickel addition and particle size reduction through ball milling: A noticeable hydrogen capacity up to 5 wt% at low temperature and pressure

*Dwi Rahmalina**, *Reza Abdu Rahman*, *Agri Suwandi*, *Ismail*

Department of Mechanical Engineering, Universitas Pancasila, Jakarta, 12640, Indonesia

HIGHLIGHTS

- High storage capacity of MgH_2 up to 5 wt% by adding 16 wt% Nickel.
- Clear evidence of the effect of moisture content in MgH_2 performance.
- A unique behavior of MgH_2 after adding 5 wt% C at specific pressure and temperature.
- Ease of process to improve MgH_2 system for large sample capacity.

GRAPHICAL ABSTRACT

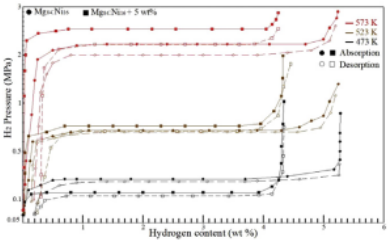

ARTICLE INFO

Article history:
Received 30 November 2019
Received in revised form
15 July 2020
Accepted 23 July 2020
Available online 17 August 2020

Keywords:
Magnesium hydride
Nickel catalyst
Carbon
Mechanical milling
Moisture content

ABSTRACT

The addition of nickel as catalyst and particle size reduction through milling process is considered as the best approach for MgH_2 properties to be thermodynamically and kinetically more favorable. The recent development in MgH_2 is done by adding Ni (14–16 wt%) and particle size reduction through simple mechanical milling at a large sample of 100 g. The research sequences are easy to adopt for the implementation and sustainable research of MgH_2. Starting from the moisture test to the milling process, continue with particle size distribution (PSD) for the milled sample and final moisture test after PSD. Some critical finding from our research includes high capacity storage of Mg_{84}:Ni_{16} above 5 wt% H_2 within 20 min at 573 K, the effect of moisture content on system performance and the different effect of carbon (C) in the system at specific temperature and pressure that may have.

* *Corresponding author.*
E-mail address: drahmalina@univpancasila.ac.id (D. Rahmalina).
https://doi.org/10.1016/j.ijhydene.2020.07.209
0360-3199/

Introduction

Solar energy is the best renewable energy option because the availability of the sun is sufficient to meet the energy consumption for the entire world [1]. The development of concentrated solar power (CSP) for harvesting solar energy is quite promising for many applications such as an electric generator or power plants, heating and cooling applications and also stored the energy in the form thermal energy is cheaper than electric [2–4]. Thermal energy storage has an essential role in CSP systems [5,6], and among the concepts of thermal energy storage, thermochemical heat storage is highly recommended because it has high energy density and long-term storage [7–9].

The metal hydride concept for thermochemical is known as the most prominent option because this model may be used for thermal storage and hydrogen storage [10,11]. Magnesium-based metal hydride (Mg) or magnesium hydride (MgH_2) is highly recommended because it has high energy density up to 2257 kJ/kg, wide operating temperature range (220 °C–550 °C), low cost, lightweight and high gravimetric capacity for hydrogen storage 7.6 wt% H_2 [12–15]. However, magnesium has poor thermodynamic properties and also slow kinetic rate during hydrogen absorption and desorption [16].

There are some methods to improve the MgH_2 system, i.e., by surface modification for the metal bulk material to promote easy chemisorption for hydride formation, adding catalysts to promote quick hydrogen sorption and lowering dehydriding temperature [17]. Nickel (Ni) is the most commonly used element as an alloy in the Mg system because it provides an excellent catalytic effect [18–21]. Many studies have shown the effect of Ni addition on MgH_2 system performance, which is summarized in Table 1. Improvement through surface modification is made by decreasing particle size through mechanical milling. The milling method is known as a cheap and appropriate method to be used on a large scale [22,23]. Table 2 shows several studies for the improvement of the MgH_2 system through the milling process.

The addition of Ni and application of ball milling provides a positive effect on the MgH_2 system. However, it still has a side effect of a reduction in H_2 storage capacity on the system. Zhang J et al. [29] revealed the latest progress on magnesium hydride system improvement and stated that the addition of Ni as a catalyst and the application of ball milling processing is the optimal method to improve MgH_2 system. The essential consideration to minimize the reduction in H_2 storage capacity is the proportion of Mg and Ni on the system [30]. For mechanical modification through the milling process, the process should be carried out through a specific set of process milling parameters in order to obtain more reliable data [31].

Although there are already many studies associated with Ni addition and particle size reduction through ball milling, the test results and analysis still show some differences. The differences are reasonable because the sample treatment, proportion and surface oxidation conditions may be different [28]. One of the most often missed factors in MgH_2 system studies is the moisture content of the tested material. Magnesium is known to be very sensitive to free air and easy to react with oxygen, forming an oxide layer that can slow down hydrogenation and dehydrogenation rate [32–35]. Another factor to be considered is the sample capacity on bed storage because it can affect the test results [36]. Furthermore, improvement and investigation of magnesium hydride also have to consider the technical aspect and production plan to reduce the cost of material processing for economically feasible [37–39].

The primary purpose of this study is to improve the thermodynamic and kinetic properties of magnesium hydride through Ni addition with a specific processing method that can be easily adapted in industry. A study showed that adding 15 wt% Ni to Mg was able to achieve maximum reversible storage up to 6 wt% [40], but it has not described how the sample was processed and the capacity of the sample. It is a good reference value for the MgH_2 system with Ni addition, however it needs to be studied further for the thermodynamic and kinetic properties of the material under clear and measurable processing steps. Hence, the study is started by measure the moisture content of the sample before the reduction of particle size through an adequate ball milling process that can be easy to be adopted in the industry. After that, testing of particle size distribution is performed to determine the grain size distribution of milled material. The milled samples are then measured for the final moisture content to be compared with the initial result to find the effect of material processing on moisture content. All samples are tested for the initial hydrogenation and dehydrogenation to find the best sample based on the kinetic rate. Finally, the best sample is characterized through pressure-composition-isotherm to assess the thermodynamic and kinetic properties in order to obtain more profound sample properties based on the thermodynamic and kinetic aspects of the sample [41,42].

Experimental procedure

Sample preparation

There are two significant parameters for processing the material, which are based on the ratio of Mg to Ni and milling parameters. The ratio used by reference is Mg_{85}:Ni_{15} by mass

Table 1 – Several reports in Mg + Ni hydride systems.

Material	Method	Results	Ref.
$Mg_{0.87}Ni_{0.13}$	Melt-spinning	Storage capacity nearly 6 wt% H_2	[20]
Mg + 10 wt% Ni + 3 wt% MgO	–	Reversible H_2 storage capacity 4.4 wt%	[21]
Mg + 20 wt% Ni hydride complex (composite)	Planetary ball mill	6.3 wt% H_2 capacity at 100 °C	[24]
Mg:$Ni_{50\text{-}33}$ wt%	Nanostructuring through mechanical grinding	H_2 capacity 1.7–2.2 wt%	[25]

Table 2 – Summary milling parameters from various research.

Material	Milling Type	Parameters	Ref.
Mg – Sb – C	ball-mill *Fritsch-Pulverisette6*	Milled under a hydrogen atmosphere, mass ratio to the ball 240	[26]
MgH_2 + NiPc and G (composite)	Ball mill	Vibrating miller, 2 h milling time, the ball to powder ration 30:1	[27]
MgH_2 + Additives	Reactive Ball Mill	Custom made ultrahigh-energy milling, milling under 150 bar hydrogen pressure, the ball to powder ratio 110:1, milling time variation: 0.5 h, 2 h, 4 h and 6 h.	[28]

ratio and variation ±1% Ni to study the effect of nickel. Commercial magnesium powder (74 μm, purity: 99.9%, Tanyun Chemical Co., Ltd.), nickel powder (63 μm, purity: 99.9%, Tanyun Chemical Co., Ltd.) were purchased and prepared by mass ratio Mg_{84}:Ni_{16}, Mg_{85}:Ni_{15} and Mg_{84}:Ni_{16}. To provide reliable data for sustainable research, the mass for each sample is 100 g.

The milling variables were milling time and ball to powder ratio because these parameters are critical variables in the milling process, especially for scale-up production, which directly affecting the results of milled material and the consumed energy during the milling process [43–45]. The milling time is set at 3 and 5 h as variation by considering the mass of material, and the final target of the milled size is 44 μm; furthermore, shorter duration also minimizes the risk of contamination [46].

A custom ring-mill with an air-cooling system for maintaining temperature during the grinding process is used. Refer to the manual and considering the size of the charge materials, the size of the milling media is Ø5 mm stainless steel ball and variation ball to powder ratio 20:1 and 30:1. The milling was taking for every 1 h and rest for 30 min to cooling down the machine and material. The milling was conducted under inert atmosphere (Ar), and stearic acid (1 wt%) was used for milling agents and then removed after milling through vacuum gas furnace. All material handling and preparation were carried out in a glove box under pure argon circulation to protect the material from oxidation and air exposure [47]. Table 3 summarizes all the prepared samples.

Experiment method

After the milling process, Particle Size Distribution (PSD) test (Mastersizer 2000, Malvern) is performed to verify the particle distribution of the milled sample. Since magnesium is very sensitive to air and oxidation, the moisture test (Mettler Toledo) is conducted before and after PSD to ensure the physical properties of the sample and provide detailed data [48–53]. The Sievert Type Apparatus is used for volumetric testing methods and activation processes to ensure more accurate results and ease in the testing process for large samples [54–57]. The apparatus is modified to enhance and maximize hydrogenation treatment for each sample. Some references relating to the testing and design process of the apparatus are used as relevant references to guarantee valid measurement values [58–60]. The void volume calibration process of bed storage and reference is done carefully and repeatedly, including for measurement instruments and data reading processes.

The initial hydrogenation and dehydrogenation test for all milled samples were carried out using the temperature-programmed method [61]. The heating rate is made constant at 5K/min with a working pressure for hydriding 5 MPa and 0.1 MPa for dehydriding and carried out within 2 h for each sample. The results of the initial tests are used to determine the best sample based on the kinetic characteristic during hydrogenation and dehydrogenation. The best sample is chosen for further measurement through Pressure-Composition-Isotherms. Considering the addition of carbon can increase desorption properties of magnesium hydride [62], we added carbon (C) 5 wt% for the best sample as a variation to investigate the influence of carbon for the selected sample performance. Before PCI measurement, the samples were activated by giving a hydrogen pressure of 5.01 MPa at 573 K and then evacuated at room temperature and repeated five times. PCI for hydrogenation and dehydrogenation is carried out at 473 K, 523 K and 573 K, both activation and PCI measurement are limited for 2 h. The selection of the temperature test based on the material characteristic and compatibility for the material application. As the additional information, the temperature also suitable for working temperature concentrated solar power parabolic trough concentrator [63], which can be used for energy input in hydrogen storage plants.

Table 3 – Sample variation according to the ratio and milling parameters.

Sample	Ratio (wt%)		Parameter Milling			
	Mg	Ni	Ball to powder ratio 20:1		Ball to powder ratio 30:1	
			3 Hours	5 Hours	3 Hours	5 Hours
S_1	86	14	√			
S_2	86	14		√		
S_3	86	14			√	
S_4	86	14				√
S_5	85	15	√			
S_6	85	15		√		
S_7	85	15			√	
S_8	85	15				√
S_9	84	16	√			
S_{10}	84	16		√		
S_{11}	84	16			√	
S_{12}	84	16				√

Result and discussion

Particle size distribution (PSD)

Mechanical milling aims to reduce the grain size of the material. It is essential to measure the final size distribution from the milled sample. Fig. 1 shows the size distribution from the milled sample with the smallest size 44 μm and shows two identical for S_1, S_3, S_5, S_7, S_9 and S_{11} (odd) compared with S_2, S_4, S_6, S_8, S_{10} and S_{12} (even). It can be seen from the milling target of 44 μm in odd samples ranging from 43.25 to 45.39 wt% and even samples from 80.02 to 86.72 wt%. Based on Table 3, the main difference between odd and even samples are in the milling time, where the even sample milled for 5 h. Thus, it can be concluded that the longer milling time is suitable for decreasing the grain size, in accordance with the literature [64].

From all samples milled for 5 h, other factors influence the achievement of 44 μm size. S_2, S_4 and S_6 show relatively lower achievement for 44 μm compared to S_8, S_{10} and S_{12}, which can be influenced by the ball to powder ratio and material proportion in the sample (Table 3). S_2, S_4 and S_6 have higher magnesium content rather than S_{10} and S_{12}, since the initial size of magnesium is 74 μm then the proportion of magnesium affects directly to the achievement of the targeted size 44 μm. There is an exception for S_6 and S_8; both samples have the same proportion but proceed with different ball to powder ratio, then it is clear to be said the higher ball to powder ratio leads to finer particle size. It can be observed from S_{10} and S_{12} where S_{12} milled with the ball to powder ratio 30:1 has finer final size than S_{10}, which milled with the ball to powder ratio 20:1. Fig. 2 shows all milled samples for 5 h.

Moisture test

Magnesium reacts with oxygen and forms magnesium oxide, which affects hydrogen to react during the hydriding process and also reduces storage capacity in magnesium. Since magnesium is very sensitive to oxygen, it is crucial to know the moisture content of the sample, especially for samples in a large amount that has a higher possibility of contamination with oxygen and air. As shown in Table 4., a single moisture test before and after the PSD test reveals a slight increase in moisture content. The overall moisture content for each sample before milling and after PSD is less than 0.3%, and the average difference is less than 0.01%. This condition indicates that the preparation and processing of the material affect the small amount for moisture content in the material [65], hence reducing the possibility of magnesium oxide formation [66]. There was no significant difference between the samples milled for 3 and 5 h; hence the effect of the milling time has not affected the increase of moisture content.

Initial hydrogenation and dehydrogenation for all samples

The hydrogenation result is shown in Fig. 3. It obviously observed that pure magnesium has the slowest kinetic rate during the hydrogenation and start to absorb hydrogen after 80 min at 670 K. The addition of nickel to the sample clearly shows a good acceleration during hydrogenation and from the graph it appears that the kinetic rate linear as the nickel content in the sample increased. The highest achievement was aimed at Mg_{84}:Ni_{16} samples (S_9 – S_{12}) with the total absorbed H_2 0.901, 0.938, 0.901, and 0.979 wt% H_2, respectively.

The dehydrogenation pattern (Fig. 4) is also identic to the hydrogenation where pure magnesium shows poor kinetic and sample with nickel has a better kinetic rate. Among all samples of Mg_{84}:Ni_{16}, S_{10} and S_{12} showed the highest absorption 0.938 and 0.979 wt% H_2. However, the graph shows that the absorption/desorption model in S_{12} experienced a sudden increase at 60 min at 590 K.

A sudden rise during hydrogenation/dehydrogenation in S_{12} (green circle in Fig. 5) makes unstable absorption and desorption of H_2, which results in shorter cycles and unstable systems for specific applications. Both samples were milled 5 h under the different ball to powder ratios, and yields were

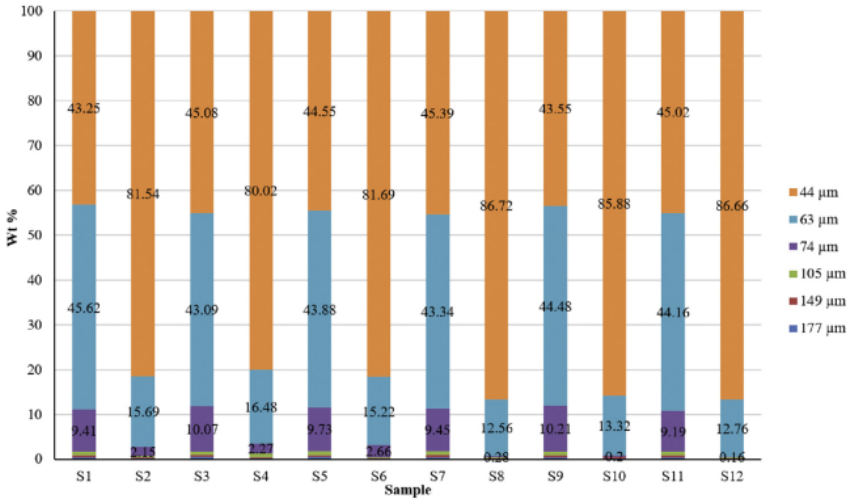

Fig. 1 – Particle size chart from the milled samples.

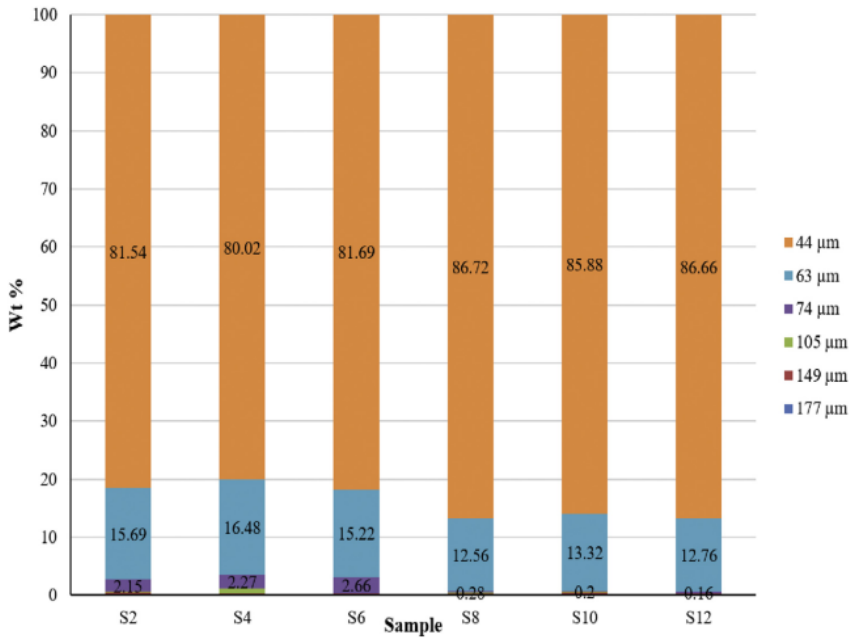

Fig. 2 – Particle size chart from sample milled for 5 h.

Table 4 – Moisture content for all sample.

Sample	Sample Ratio (Mg:Ni)	% Moisture Content (MC)		Δ_{MC}
		Before Milling	After PSD	
S_1	86:14	0.176	0.188	0.012
S_2	86:14	0.177	0.189	0.012
S_3	86:14	0.180	0.191	0.011
S_4	86:14	0.182	0.190	0.008
S_5	85:15	0.281	0.285	0.004
S_6	85:15	0.282	0.291	0.009
S_7	85:15	0.285	0.290	0.005
S_8	85:15	0.281	0.289	0.008
S_9	84:16	0.189	0.201	0.012
S_{10}	84:16	0.183	0.191	0.008
S_{11}	84:16	0.191	0.197	0.006
S_{12}	84:16	0.195	0.202	0.007
Average %MC		0.217	0.225	0.0085

slightly different for particle sizes 44 and 63 µm where S_{10} had 85.88% and 13.32% and for S_{12} are 86.66% and 12.76%, respectively (Fig. 3). Therefore, there is no direct effect due to particle size differences. Another consideration is the moisture content (Table 4) in the as milled S_{12} (0.202%) is higher than as milled S_{10} (0.191%). Higher moisture content in S_{12} is the factor that affects the instability phenomenon during hydrogenation/dehydrogenation, and it can only be observed under a large sample (100 g). The O_2 exposure causes the formation of the oxide layer on the metal surface, and it creates a barrier for the hydrogen molecules to penetrate the bulk material. When the pressure from the hydrogen molecule reaches the saturated point and strengthened by nickel, which produces a more substantial penetration effect on the surface, the oxide layer will break, and the reaction of hydride formation is too fast, causing a sudden release of heat around the bulk material. This phenomenon proves the importance of measuring moisture content in samples that are sensitive to air contamination to avoid misinterpretation reading of the hydriding/dehydriding result.

Further observations for microstructural and morphological in S_{10} and S_{12} aim to see the effects of the initial hydrogenation and dehydrogenation. Each sample was compared before and after hydriding (Fig. 6). As shown in S_{12}, after dehydriding, there are several visible forms of porous (red circled), the cause of this porous can be attributed to the sudden rise in the sample during the hydriding and dehydriding process.

Activation for the best sample

Two new samples are prepared for PCI measurement, as milled $Mg_{84}Ni_{16}$ and as milled $Mg_{84}Ni_{16}$ + 5 wt% C (10 µm). The purpose of adding carbon is to provide variations in the characterization of the Mg:Ni system because, in some reports, the addition of carbon as a composite for the MgH_2 system has a good influence on thermal conductivity and also dehydrogenation rate [67–69]. The addition of carbon is limited to only 5 wt% to avoid decreasing kinetic hydrogenation [70]. The samples are activated before PCI measurements. The activation process is carried out by introducing a hydrogen pressure of 5.01 MPa for 2 h. The temperature is 573.15 K and kept constant during the process. The goal for the activation process is to remove gases or liquids that may still be present in the system and also to

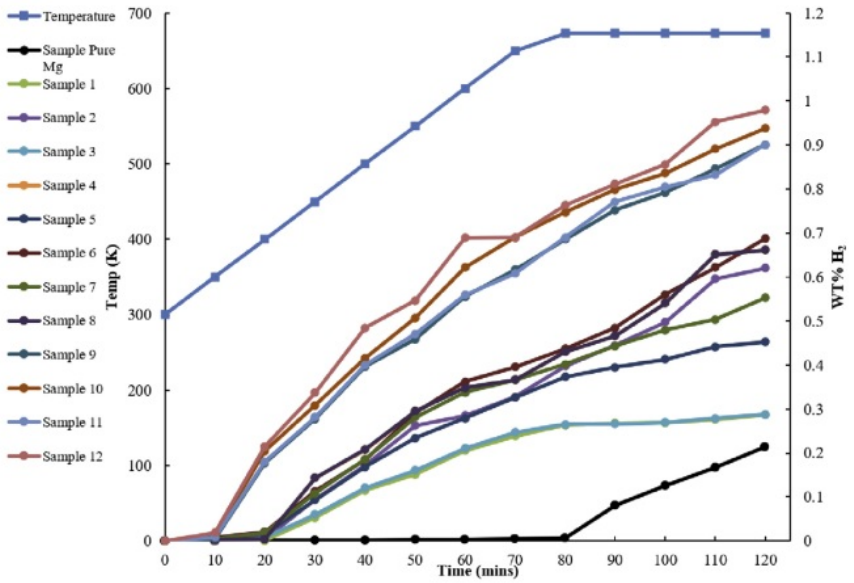

Fig. 3 – TPD hydrogenation for all samples.

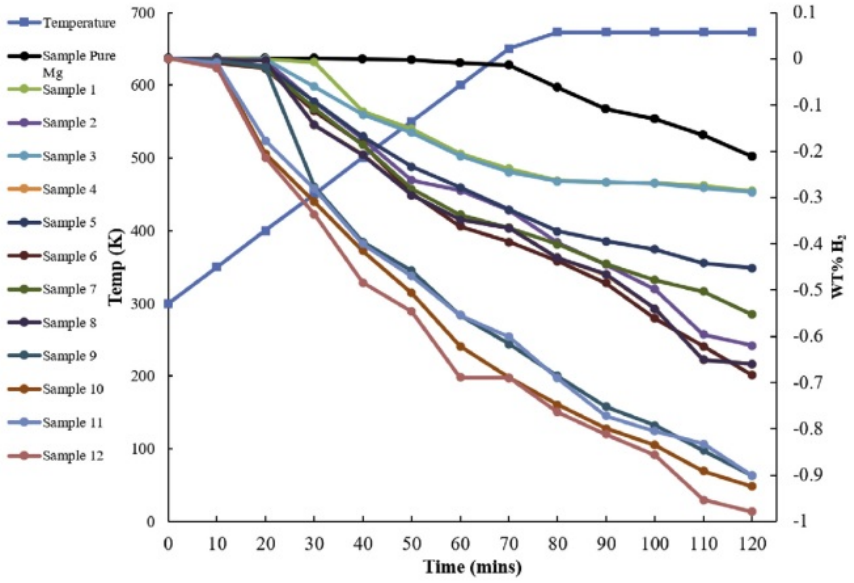

Fig. 4 – TPD dehydrogenation for all samples.

weaken the oxide layer and improve the hydrogenation process.

From the graphical model in Fig. 7, there is a higher absorption surge between the 3rd to the 4th cycle. For instance, Mg_{84}:Ni_{16} absorbed 2.17 wt% H_2 at the end of the 3rd cycle and leap to 3.13 wt% at the end of the 4th cycle, the same phenomenon was observed from Mg_{84}:Ni_{16} + 5 wt% C. It appears due to a significant elastic effect caused by mutual influence from each particle during phase changing ($\alpha \rightarrow \beta$ phase), and it does not appear in smaller sample sizes [71]. The activation and degasification cause the sample to prepare a better hydrogen dissociation, and from Fig. 7 shows that absorption capacity increases as the cycle repeated. The change in absorption capacity from the 4th to the 5th cycle is not very significant compared to the previous cycle. The addition of carbon to Mg_{84}:Ni_{16} made a slight decrease in for the absorbed H_2 but does not have a significant effect on the rate of kinetic reaction. As a special note, the void volume of the bed reactor is carefully checked after each cycle done to avoid misreading

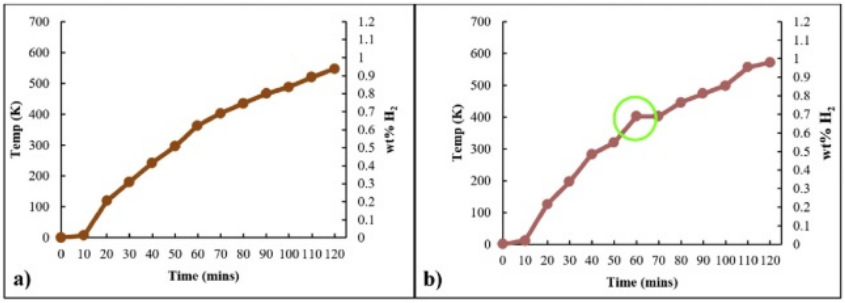

Fig. 5 – Hydrogenation model for S_{10} (a) and S_{12} (b).

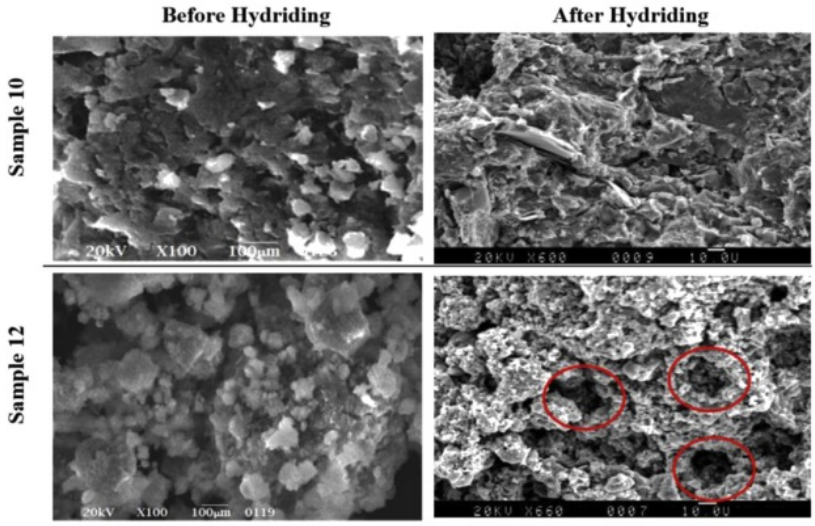

Fig. 6 – SEM micrograph for S_{10} and S_{12}.

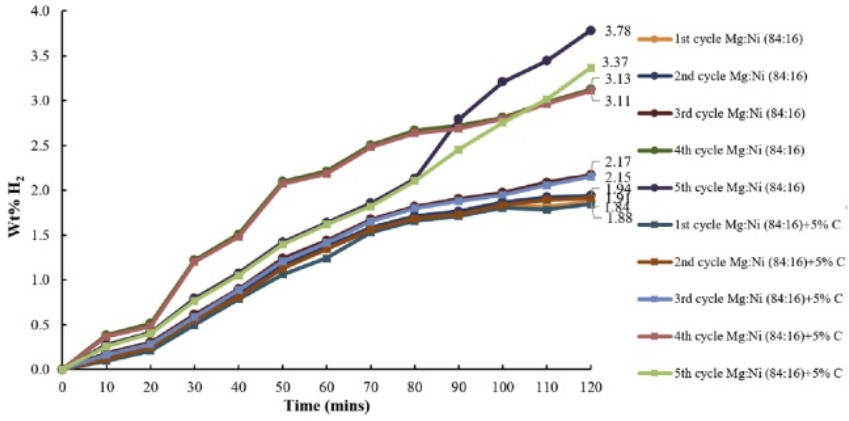

Fig. 7 – Graphical model from activation result.

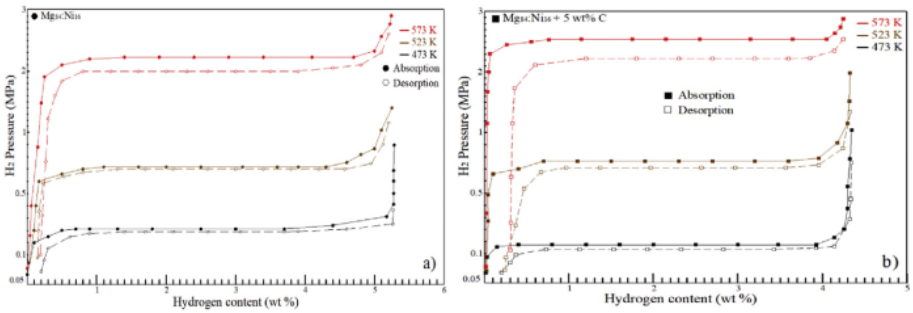

Fig. 8 – Absorption and desorption PCI curve for Mg_{84}:Ni_{16} (a) and Mg_{84}:Ni_{16} + 5 wt% C (b).

the measurement results caused by deformation in reactor geometry due to the activation process.

Pressure-composition-isotherm

The result from PCI measurements for Mg_{84}:Ni_{16} and Mg_{84}:Ni_{16} + 5 wt% C are shown in Fig. 8. The straight line on the graph shows the plateau pressure, and it indicates the existence of the α–phase (solid solution) and β–phase (hydride solution). The increase in temperature is followed by an increase in hydrogen pressure and also affects the shorter plateau line, which means the less hydrogen capacity absorbed by the sample. The shorter the plateau, the shorter the formation of the transition phase (α + β phase), so the total absorbed hydrogen decreases and lead to a quicker hydride solution.

Equilibrium pressure at 473 K for each sample occurs at relatively low pressure. The equilibrium pressure for Mg_{14}:Ni_{16} and Mg_{84}:Ni_{16} + 5 wt% C are 0.206 MPa and 0.179, respectively. Low equilibrium pressure during absorption and desorption is a significant achievement that only occur in samples with larger capacity in agreement with the literature [71]. The reduction is supported by the use of multi-porous tubes and combined heating system in bed reactor to promote a better heat and hydrogen distribution to the sample, consequently the sample able to achieve equilibrium pressure at relatively lower pressure and temperature. It makes a higher hydrogen absorption in the sample at lower temperatures where Mg_{84}:Ni_{16} is 5.29 wt% H_2 and Mg_{84}:Ni_{16} + 5 wt% C 4.37 wt% H_2.

The addition of carbon directly impacts the reduction of the absorbed H_2 amount of the sample, and also from the graph, it can be observed that the hysterical loss sample with carbon is higher. Hysteresis loss is unfavorable on the hydride system due to the lower desorption pressure compared to absorption, and it is not desirable for practical applications. Data from PCI measurement is used to make the Van not Hoff plot to estimate enthalpy and entropy formation for the hydride formation. Fig. 9 shows the Van't Hoff plot graph for both samples, and all values related to the PCI measurement results are summarized in Table 5.

The enthalpy and entropy formation of Mg_{84}:Ni_{16} and the storage capacity generally is better than most reported research in MgNi system, especially in this study the reduction of particle size through ball milling is simply made without reaching nano size. It is an important finding related to the development of magnesium hydride as a hydrogen storage material with the addition of nickel as a catalyst to improve the performance of MgH_2. There two keys factor that needs to be considered, first the material treatment and handling must pay attention to the moisture content that has an impact on the hydriding process, second is the bed storage for hydriding/dehydriding must be able to provide sufficient distribution of the H_2 and heat to the materials; thus the actual properties and characteristic of the material can be more clearly understanding.

The desorption pressure drop is seen in Fig. 9(b) for Mg_{84}:Ni_{16} + 5 wt% C where the desorption slope is below the absorption plot, yields a significant increase for enthalpy and entropy formation during desorption. In contrast to that, Mg_{84}:Ni_{16} shows the desorption slope is slightly lower than the absorption slope. Changes in the absorption capacity and equilibrium pressure cause an increase in the values of ΔH and ΔS from samples with carbon, which directly affects the

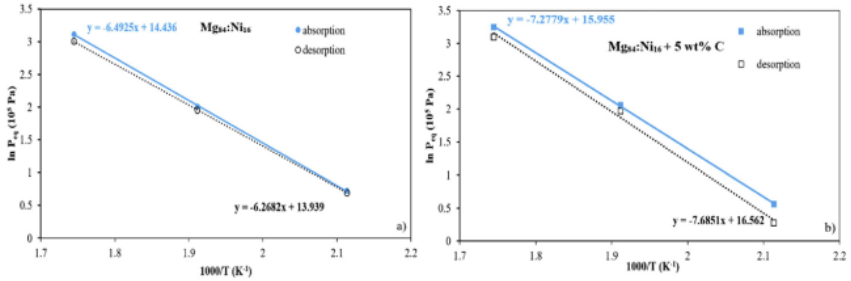

Fig. 9 – Van't Hoff plot from PCI for Mg_{84}:Ni_{16} (a) and Mg_{84}:Ni_{16} + 5 wt% C (b).

Table 5 – Calculated thermodynamic properties from PCI measurements.

Sample	T	P_{abs}	P_{des}	ΔH_{abs}	ΔH_{des}	ΔS_{abs}	ΔS_{des}	Hysteresis Loss
	(K)	Pressure Equilibrium (MPa)		(kJ/mol)	(kJ/mol)	(J/mol.K)	(J/mol.K)	(kJ/mol)
Mg_{84}:Ni_{16}	473	0.206	0.199					0.06798
	523	0.745	0.704	−53.98	52.28	120.02	115.89	0.12307
	553	2.258	2.018					0.25832
Mg_{84}:Ni_{16} + 5 wt% C	473	0.179	0.131					0.61384
	523	0.786	0.720	−60.51	63.89	132.65	137.69	0.19068
	553	2.569	2.211					0.33461

stability of the hydride formed, and thus the decomposition of the hydride requires higher energy. There is a unique characteristic for the hysteresis loss value in Mg_{84}:Ni_{16} + 5 wt% C where the hysteresis loss is not linear concerning an increase in temperature (in Mg_{84}:Ni_{16} is linear) where at a temperature of 523 K the hysteresis loss value decreases. In MgH_2 system, carbon acts merely as a simple scaffold, and there is no reaction between metal hydride and carbon during the synthesis process, the different value of hysteresis loss at 523 K can be used as a special consideration to find an association between the thermodynamic consideration of the additional carbon in MgH_2 system.

After thermodynamic evaluation from PCI measurement, the kinetic properties of the sample need to describe in order to study the sample performance in terms of how quickly the sample able to absorb and desorb hydrogen. Fig. 10 shows the hydrogenation for both samples and it is clear to note that as the temperature increase, the kinetic rate will increase. Mg_{84}:Ni_{16} shows an excellent performance where it can absorb hydrogen at lower temperatures, and it is evidently the effect of nickel as catalyst changed the pathway during the hydriding process. In contrast, during hydrogenation sample with carbon has a slower rate compared to Mg_{84}:Ni_{16}.

It can be seen from Fig. 11, Mg_{84}:Ni_{16} + 5 wt% C shows different performance during the dehydriding process. The kinetic rate during the dehydrogenation process in the sample with carbon is quicker compared to during hydrogenation, and the increase in temperature also accelerates the kinetic, in good agreement with [72]. The drawback due to carbon addition is decreased the desorbed H_2 as the temperature increase, which is proven the impact of hysteresis loss. Table 6 shows distinctly that temperature rises is accompanied by a decrease in percent effective storage, apart from that, sample Mg_{84}:Ni_{16} 5 wt% C at 523 K has a higher effective capacity than 473 K. According to Table 5 where hysteresis loss at 523 K for Mg_{84}:Ni_{16} 5 wt% C decreased, it has a direct effect on the effective storage capacity. Again, it reinforces that there is an interrelationship between the effect of temperature and pressure on Mg_{84}:Ni_{16} + 5 wt% C that only occurs at certain temperatures and pressures.

Apart from the decrease in capacity due to hysteresis loss, all samples have effective storage above 95%. Referring to

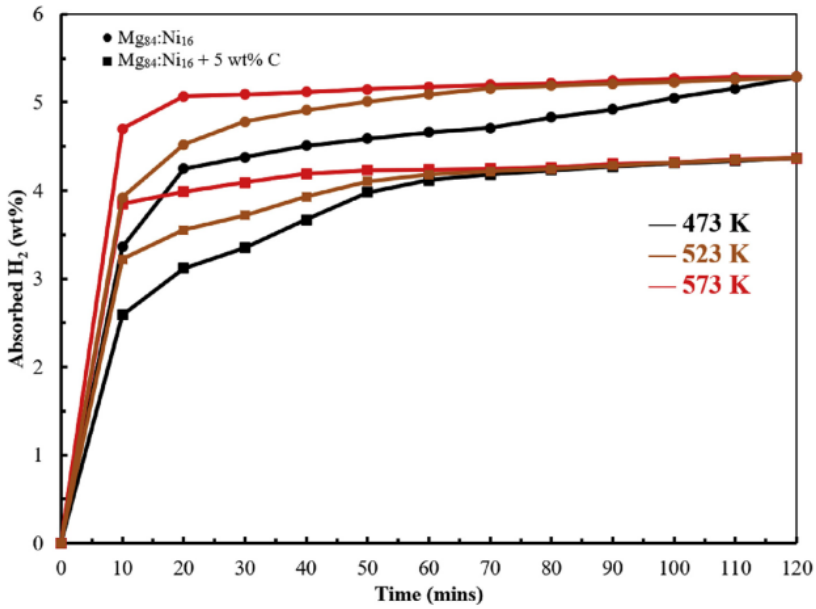

Fig. 10 – Hydrogenation for Mg_{84}:Ni_{16} and Mg_{84}:Ni_{16} + 5 wt% C.

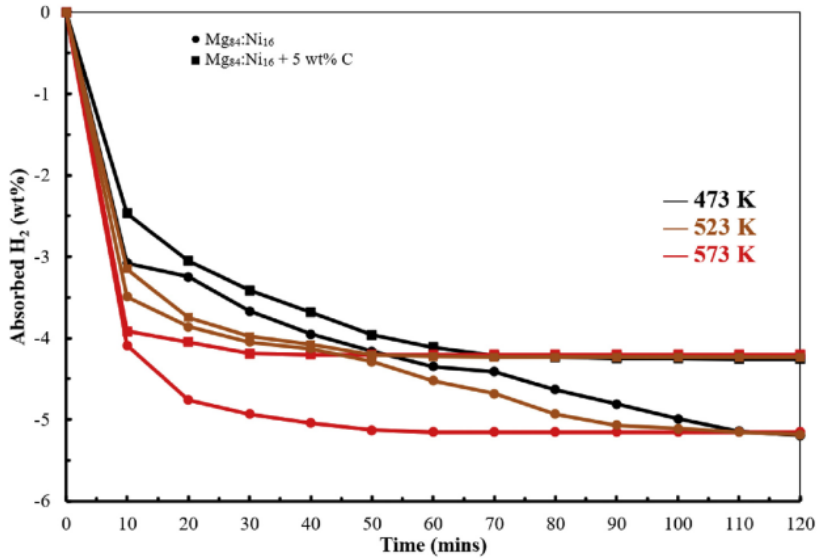

Fig. 11 – Dehydrogenation for Mg_{84}:Ni_{16} and Mg_{84}:Ni_{16} + 5 wt% C.

Table 6 – Comparison for absorbed and desorbed H_2 at specific temperature.

Sample	T (K)	wt% H_2		% effective H_2 storage
		Hydrogenation	Dehydrogenation	
Mg_{84}:Ni_{16}	473	5.29	−5.19	98.1
	523	5.29	−5.18	97.9
	553	5.29	−5.15	97.3
Mg_{84}:Ni_{16} + 5 wt% C	473	4.37	−4.26	97.5
	523	4.37	−4.28	97.9
	553	4.37	−4.20	96.1

kinetic considerations, the addition of Ni by 16 wt% to the Mg system has an excellent catalyst effect, which increases the hydrogenation and dehydrogenation rates. The addition of Ni by 16% also helps improve thermodynamic properties where the enthalpy of formation is decreased while keep maintaining storage capacity above 5 wt%. Special consideration was found with the addition of carbon by 5 wt%, which had an excellent dehydrogenation effect but had an impact on reducing the hydrogenation rate and storage capacity. One important thing needs to be investigated further related to the relationship between carbon and system temperature and pressure because at temperature 523 K the addition of carbon shows quite different characteristics, primarily related to lower hysteresis loss; lower than the same sample at temperatures 473 K and 573 K.

Conclusions

This study shows the recent developments for the improvement of the MgH_2 system by decreasing grain size and adding nickel as a catalyst. Although there have been many reports related to these two efforts, most of the method reported is less economically feasible and limited to a small sample capacity. An important finding from this study shows that the importance of measuring moisture content in samples (especially magnesium based) because moisture content can be a factor that influences the nature of the sample when characterized. We limit the nickel addition in the range of 14–16% and show the pattern the kinetic rate is increased as well as the increase of nickel content. The most important thing that can be obtained through this study is the achievement of the absorption capacity of hydrogen in the Mg_{84}:Ni_{16}, which can absorb hydrogen above 5 wt% through a simple reduction in grain size without nanosizing, though the final capacity of the sample is lower than the reference. The application of proper bed storage that enriches the hydrogen distribution through the sample provides a better heat transfer, and a large sample capacity can be used as a consideration to determine the actual performance of the MgH_2 system. In particular, further research is needed to find the relationship between carbon and pressure and temperature about the effect of carbon on the thermodynamic nature of the system. Further research needs to consider testing the cycle of Mg_{84}:Ni_{16} and also in different Ni ranges.

Declaration of competing interest

The authors declare that they have no known competing financial interests or personal relationships that could have appeared to influence the work reported in this paper.

Acknowledgement

The authors are grateful to The Ministry of Research, Technology and Higher Education of the Republic of Indonesia by funding this study under the Magister Research Incentive 2019.

REFERENCES

[1] Bijarniya JP, Sudhakar K, Baredar P. Concentrated solar power technology in India: a review. Renew Sustain Energy Rev 2016;63:593–603. https://doi.org/10.1016/j.rser.2016.05.064.
[2] Singh A, Khaewhom S, Kaistha N. Design and control of a small-scale isolated concentrated solar power generation unit. Ind Eng Chem Res 2018;57:623–38. https://doi.org/10.1021/acs.iecr.7b02748.
[3] Prieto C, Cooper P, Fernández AI, Cabeza LF. Review of technology: thermochemical energy storage for concentrated solar power plants. Renew Sustain Energy Rev 2016;60:909–29. https://doi.org/10.1016/j.rser.2015.12.364.
[4] Narayanan S, Li X, Yang S, Kim H, Umans A, McKay IS, et al. Thermal battery for portable climate control. Appl Energy 2015;149:104–16. https://doi.org/10.1016/j.apenergy.2015.03.101.
[5] Eslami M, Bahrami MA. Sensible and latent thermal energy storage with constructal fins. Int J Hydrogen Energy 2017;42:17681–91. https://doi.org/10.1016/j.ijhydene.2017.04.097.
[6] Elbahjaoui R, El Qarnia H. Performance evaluation of a solar thermal energy storage system using nanoparticle-enhanced phase change material. Int J Hydrogen Energy 2019;44:2013–28. https://doi.org/10.1016/j.ijhydene.2018.11.116.
[7] Chacartegui R, Alovisio A, Ortiz C, Valverde JM, Verda V, Becerra JA. Thermochemical energy storage of concentrated solar power by integration of the calcium looping process and a CO2 power cycle. Appl Energy 2016;173:589–605. https://doi.org/10.1016/j.apenergy.2016.04.053.
[8] d'Entremont A, Corgnale C, Hardy B, Zidan R. Simulation of high temperature thermal energy storage system based on coupled metal hydrides for solar driven steam power plants. Int J Hydrogen Energy 2018;43:817–30. https://doi.org/10.1016/j.ijhydene.2017.11.100.
[9] Nyamsi SN, Lototskyy M, Tolj I. Selection of metal hydrides-based thermal energy storage: energy storage efficiency and density targets. Int J Hydrogen Energy 2018;43:22568–83. https://doi.org/10.1016/j.ijhydene.2018.10.100.
[10] Gambini M, Stilo T, Vellini M, Montanari R. High temperature metal hydrides for energy systems Part A: numerical model validation and calibration. Int J Hydrogen Energy 2017;42:16195–202. https://doi.org/10.1016/j.ijhydene.2017.05.062.
[11] d'Entremont A, Corgnale C, Sulic M, Hardy B, Zidan R, Motyka T. Modeling of a thermal energy storage system based on coupled metal hydrides (magnesium iron – sodium alanate) for concentrating solar power plants. Int J Hydrogen Energy 2017;42:22518–29. https://doi.org/10.1016/j.ijhydene.2017.04.231.
[12] Fang ZZ, Zhou C, Fan P, Udell KS, Bowman RC, Vajo JJ, et al. Metal hydrides based high energy density thermal battery. J Alloys Compd 2015;645:S184–9. https://doi.org/10.1016/j.jallcom.2014.12.260.
[13] Sheppard DA, Buckley CE. The potential of metal hydrides paired with compressed hydrogen as thermal energy storage for concentrating solar power plants. Int J Hydrogen Energy 2019;44:9143–63. https://doi.org/10.1016/j.ijhydene.2019.01.271.
[14] Zhou C, Fang ZZ, Lu J, Zhang X. Thermodynamic and kinetic destabilization of magnesium hydride using Mg-In solid solution alloys. J Am Chem Soc 2013;135. https://doi.org/10.1021/ja4058794. 10982–5.
[15] Liu X, Yin S, Lan Q, Xue J, Le Q, Zhang Z. Investigation of the hydrogen states in magnesium alloys and their effects on mechanical properties. Mater Des 2017;134:446–54. https://doi.org/10.1016/j.matdes.2017.08.073.
[16] Vijay Babu AR, Devunuri N, Manisha DR, Prashanthi Y, Merugu R, Ravi Teja AJR. Magnesium hydrides for hydrogen storage: a mini review. Int J Chem Res 2014;6:3451–5.
[17] Sakintuna B, Lamari-Darkrim F, Hirscher M. Metal hydride materials for solid hydrogen storage: a review. Int J Hydrogen Energy 2007;32:1121–40. https://doi.org/10.1016/j.ijhydene.2006.11.022.
[18] Schlapbach L, Züttel A. Hydrogen-storage materials for mobile applications. Nature 2001;414:353–8. https://doi.org/10.1038/35104634.
[19] Fernández JF, Sánchez CR. Simultaneous TDS-DSC measurements in magnesium hydride. J Alloys Compd 2003;356(357):348–52. https://doi.org/10.1016/S0925-8388(02)01228-8.
[20] Friedlmeier G, Arakawa M, Hirai T, Akiba E. Preparation and structural, thermal and hydriding characteristics of melt-spun Mg-Ni alloys. J Alloys Compd 1999;292:107–17. https://doi.org/10.1016/S0925-8388(99)00285-6.
[21] Callini E, Pasquini L, Jensen TR, Bonetti E. Hydrogen storage properties of Mg-Ni nanoparticles. Int J Hydrogen Energy 2013;38:12207–12. https://doi.org/10.1016/j.ijhydene.2013.05.139.
[22] Shikin IV, Elets DI, Voyt AP, Gabis IE. Activation of magnesium hydride by pressing with catalytic additives. Tech Phys Lett 2017;43:190–3. https://doi.org/10.1134/S1063785017020262.
[23] Ney C, Kohlmann H, Kickelbick G. Metal hydride synthesis through reactive milling of metals with solid acids in a planetary ball mill. Int J Hydrogen Energy 2011;36:9086–90. https://doi.org/10.1016/j.ijhydene.2011.04.191.
[24] Galey B, Auroux A, Sabo-Etienne S, Dhaher S, Grellier M, Postole G. Improved hydrogen storage properties of Mg/MgH2 thanks to the addition of nickel hydride complex precursors. Int J Hydrogen Energy 2019;44:28848–62. https://doi.org/10.1016/j.ijhydene.2019.09.127.
[25] Orimo S, Ikeda K, Hujii H, Fujikawa Y, Kitano Y, Yamamoto K. Structural and hydriding properties Mg-Ni-H system with nano- and/or amorphous structures. Acta Mater 1997;45:2271–8.
[26] Cermak J, Kral L, Roupcova P. Improvement of hydrogen storage kinetics in ball-milled magnesium doped with antimony. Int J Hydrogen Energy 2017;42:6144–51. https://doi.org/10.1016/j.ijhydene.2016.11.113.
[27] Zhang J, Qu H, Yan S, Wu G, Yu XF, Zhou DW. Catalytic effect of nickel phthalocyanine on hydrogen storage properties of magnesium hydride: experimental and first-principles studies. Int J Hydrogen Energy 2017;42:28485–97. https://doi.org/10.1016/j.ijhydene.2017.09.170.

[28] Li J, Zhou C, Fang ZZ, Bowman RC, Lu J, Ren C. Isothermal hydrogenation kinetics of ball-milled nano-catalyzed magnesium hydride. Materialia 2019;5:100227. https://doi.org/10.1016/j.mtla.2019.100227.
[29] Zhang J, Yan S, Qu H. Recent progress in magnesium hydride modified through catalysis and nanoconfinement. Int J Hydrogen Energy 2018;43:1545–65. https://doi.org/10.1016/j.ijhydene.2017.11.135.
[30] Crivello JC, Denys RV, Dornheim M, Felderhoff M, Grant DM, Huot J, et al. Mg-based compounds for hydrogen and energy storage. Appl Phys A Mater Sci Process 2016;122:1–17. https://doi.org/10.1007/s00339-016-9601-1.
[31] Huot J, Liang G, Boily S, Van Neste A, Schulz R. Structural study and hydrogen sorption kinetics of ball-milled magnesium hydride. J Alloys Compd 1999;293:495–500. https://doi.org/10.1016/S0925-8388(99)00474-0.
[32] Malka IE, Bystrzycki J. The effect of storage time on the thermal behavior of nanocrystalline magnesium hydride with metal halide additives. Int J Hydrogen Energy 2014;39:3352–9. https://doi.org/10.1016/j.ijhydene.2013.12.100.
[33] Zhou S, Zhang X, Li T, Wang N, Chen H, Zhang T, et al. Nano-confined magnesium for hydrogen storage from reactive milling with anthracite carbon as milling aid. Int J Hydrogen Energy 2014;39:13628–33. https://doi.org/10.1016/j.ijhydene.2014.02.092.
[34] Sevastyanova LG, Genchel VK, Klyamkin SN, Larionova PA, Bulychev BM. Hydrogen generation by oxidation of "mechanical alloys" of magnesium with iron and copper in aqueous salt solutions. Int J Hydrogen Energy 2017;42:16961–7. https://doi.org/10.1016/j.ijhydene.2017.05.242.
[35] Tegel M, Schöne S, Kieback B, Röntzsch L. An efficient hydrolysis of MgH2-based materials. Int J Hydrogen Energy 2017;42:2167–76. https://doi.org/10.1016/j.ijhydene.2016.09.084.
[36] Borzenko VI, Romanov IA, Dunikov DO, Kazakov AN. Hydrogen sorption properties of metal hydride beds: effect of internal stresses caused by reactor geometry. Int J Hydrogen Energy 2019;44:6086–92. https://doi.org/10.1016/j.ijhydene.2019.01.052.
[37] Corgnale C, Hardy B, Motyka T, Zidan R. Metal hydride based thermal energy storage system requirements for high performance concentrating solar power plants. Int J Hydrogen Energy 2016;41:20217–30. https://doi.org/10.1016/j.ijhydene.2016.09.108.
[38] Potapov SN, Gvozdkov IA, Belyaev VA, Verbetsky VN, Mitrokhin SV. Magnesium hydride based hydrogen chemical source: development and application perspectives. Int J Hydrogen Energy 2019;44:28578–85. https://doi.org/10.1016/j.ijhydene.2019.09.094.
[39] Delhomme B, Lanzini A, Ortigoza-Villalba GA, Nachev S, De Rango P, Santarelli M, et al. Coupling and thermal integration of a solid oxide fuel cell with a magnesium hydride tank. Int J Hydrogen Energy 2013;38:4740–7. https://doi.org/10.1016/j.ijhydene.2013.01.140.
[40] Crivello JC, Dam B, Denys RV, Dornheim M, Grant DM, Huot J, et al. Review of magnesium hydride-based materials: development and optimisation. Appl Phys A Mater Sci Process 2016;122:1–20. https://doi.org/10.1007/s00339-016-9602-0.
[41] Sharma VK, Kumar Anil E. Measurement and simulation of hydrogen storage and thermodynamic properties of LaNi4.7Al0.3 hydride. Int J Appl Eng Res 2014;9:985–94.
[42] Anil Kumar E, Prakash Maiya M, Srinivasa Murthy S. Influence of transient operating conditions on pressure-concentration isotherms and storage characteristics of hydriding alloys. Int J Hydrogen Energy 2007;32:2382–9. https://doi.org/10.1016/j.ijhydene.2006.10.041.
[43] Prasad Yadav T, Manohar Yadav R, Pratap Singh D. Mechanical milling: a top down approach for the synthesis of nanomaterials and nanocomposites. Nanosci Nanotechnol 2012;2:22–48. https://doi.org/10.5923/j.nn.20120203.01.
[44] Alsabawi K, Gray EMA, Webb CJ. The effect of ball-milling gas environment on the sorption kinetics of MgH 2 with/without additives for hydrogen storage. Int J Hydrogen Energy 2019;44:2976–80. https://doi.org/10.1016/j.ijhydene.2018.12.026.
[45] Pantić T, Milanović I, Lukić M, Grbović Novaković J, Kurko S, Biliškov N, et al. The influence of mechanical milling parameters on hydrogen desorption from Mgh2-Wo3 composites. Int J Hydrogen Energy 2020;45:7901–11. https://doi.org/10.1016/j.ijhydene.2019.07.167.
[46] Suryanarayana C. Mechanical alloying and milling. Prog Mater Sci 2001;46:1–184. https://doi.org/10.1016/S0079-6425(99)00010-9.
[47] Dong D, Humphries TD, Sheppard DA, Stansby B, Paskevicius M, Sofianos MV, et al. Thermal optimisation of metal hydride reactors for thermal energy storage applications. Sustain Energy Fuels 2017;1:1820–9. https://doi.org/10.1039/c7se00316a.
[48] Faqih AMN, Mehrotra A, Hammond SV, Muzzio FJ. Effect of moisture and magnesium stearate concentration on flow properties of cohesive granular materials. Int J Pharm 2007;336:338–45. https://doi.org/10.1016/j.ijpharm.2006.12.024.
[49] Chao CH, Jen TC. Reaction of magnesium hydride with water to produce hydrogen. Appl Mech Mater 2013;302:151–7. https://doi.org/10.4028/www.scientific.net/AMM.302.151.
[50] Elhamshri FAM, Kayfeci M. Enhancement of hydrogen charging in metal hydride-based storage systems using heat pipe. Int J Hydrogen Energy 2019:18927–38. https://doi.org/10.1016/j.ijhydene.2018.10.040.
[51] Tian M, Shang C. Mg-based composites for enhanced hydrogen storage performance. Int J Hydrogen Energy 2019:338–44. https://doi.org/10.1016/j.ijhydene.2018.02.119.
[52] Beatrice CAG, Moreira BR, de Oliveira AD, Passador FR, de Almeida Neto GR, Leiva DR, et al. Development of polymer nanocomposites with sodium alanate for hydrogen storage. Int J Hydrogen Energy 2020;45:5337–46. https://doi.org/10.1016/j.ijhydene.2019.06.169.
[53] Dehouche Z, Goyette J, Bose TK, Schulz R. Moisture effect on hydrogen storage properties of nanostructured MgH2-V-Ti composite. Int J Hydrogen Energy 2003;28:983–8. https://doi.org/10.1016/S0360-3199(02)00196-9.
[54] Chaise A, De Rango P, Marty P, Fruchart D. Experimental and numerical study of a magnesium hydride tank. Int J Hydrogen Energy 2010;35:6311–22. https://doi.org/10.1016/j.ijhydene.2010.03.057.
[55] Tanniru M, Tien HY, Ebrahimi F. Study of the dehydrogenation behavior of magnesium hydride. Scripta Mater 2010;63:58–60. https://doi.org/10.1016/j.scriptamat.2010.03.019.
[56] Brestovič T, Jasminská N, Lázár M, Dobáková R. Measurement of operating parameters of a hydrogen compressor using metal hydride materials. MATEC Web Conf 2018;168. https://doi.org/10.1051/matecconf/201816806002.
[57] Mazzoli M. Technical assessment of compressed hydrogen storage tank systems for automotive applications, vol. 85; 2005. https://doi.org/10.1007/s00712-005-0133-y.
[58] Broom DP. Hydrogen sorption measurements on potential storage materials. https://doi.org/10.2790/86100; 2008.
[59] Sharma VK, Anil Kumar E. Effect of measurement parameters on thermodynamic properties of La-based metal

hydrides. Int J Hydrogen Energy 2014;39:5888–98. https://doi.org/10.1016/j.ijhydene.2014.01.174.
[60] Gross KJ, Technology H, Llc C. Best practices for the characterization of hydrogen storage materials preface. 2008.
[61] Auroux A. Calorimetry and thermal methods in catalysis, vol. 154; 2013. https://doi.org/10.1007/978-3-642-11954-5.
[62] Abdul Majid NA, Maeda N, Notomi M. Improved hydrogen desorption properties of magnesium hydride with TiFe0.8Mn0.2, graphite and iron addition. Int J Hydrogen Energy 2019;44:29189–95. https://doi.org/10.1016/j.ijhydene.2019.02.190.
[63] Simsek Y, Watts D, Escobar R. Sustainability evaluation of concentrated solar power (CSP) projects under clean development mechanism (CDM) by using multi criteria decision method (MCDM). Renew Sustain Energy Rev 2018;93:421–38. https://doi.org/10.1016/j.rser.2018.04.090.
[64] Zhang DL. Processing of advanced materials using high-energy mechanical milling. Prog Mater Sci 2004;49:537–60. https://doi.org/10.1016/S0079-6425(03)00034-3.
[65] Liu J, Schaef HT, Martin PF, McGrail BP, Fifield LS. Understanding H2 evolution from the decomposition of dibutylmagnesium isomers using in-situ X-ray diffraction coupled with mass spectroscopy. ACS Appl Energy Mater 2019;2:5272–8. https://doi.org/10.1021/acsaem.9b00958.
[66] Bhouri M, Bürger I. Numerical investigation of H2 absorption in an adiabatic high-temperature metal hydride reactor based on thermochemical heat storage: MgH2 and Mg(OH)2 as reference materials. Int J Hydrogen Energy 2017;42:16632–44. https://doi.org/10.1016/j.ijhydene.2017.05.123.
[67] Wu CZ, Wang P, Yao X, Liu C, Chen DM, Lu GQ, et al. Effect of carbon/noncarbon addition on hydrogen storage behaviors of magnesium hydride. J Alloys Compd 2006;414:259–64. https://doi.org/10.1016/j.jallcom.2005.07.021.
[68] Peng D, Li Y, Liu Y, Zhang L, Zhang H, Ding Z, et al. Effect of LiBH4 on hydrogen storage properties of magnesium hydride-carbon composite. J Alloys Compd 2017;711:104–10. https://doi.org/10.1016/j.jallcom.2017.03.263.
[69] Klimkowicz A, Takasaki A, Gondek Ł, Figiel H, wierczek K. Hydrogen desorption properties of magnesium hydride catalyzed multiply with carbon and silicon. J Alloys Compd 2015;645:S80–3. https://doi.org/10.1016/j.jallcom.2015.01.178.
[70] Shang H, Li Y, Zhang Y, Wei X, Qi Y, Zhao D. Influences of adding nano-graphite powders on microstructure and gaseous hydrogen storage properties of ball milled Mg90Al10 alloy. Carbon N Y 2019;149:93–104. https://doi.org/10.1016/j.carbon.2019.04.028.
[71] Malyshenko SP, Mitrokhin SV, Romanov IA. Effects of scaling in metal hydride materials for hydrogen storage and compression. J Alloys Compd 2015;645:S84–8. https://doi.org/10.1016/j.jallcom.2014.12.273.
[72] Yao X, Lu G. Magnesium-based materials for hydrogen storage: recent advances and future perspectives. Chin Sci Bull 2008;53:2421–31. https://doi.org/10.1007/s11434-008-0325-2.

The recent development on MgH system by 16 wt% nickel addition and particle size reduction through ball milling: A noticeable hydrogen capacity up to 5 wt% at low temperature and pressure

ORIGINALITY REPORT

4%	3%	4%	3%
SIMILARITY INDEX	INTERNET SOURCES	PUBLICATIONS	STUDENT PAPERS

PRIMARY SOURCES

1	Submitted to School of Business and Management ITB Student Paper	1%
2	Submitted to King Mongkut's Institute of Technology Ladkrabang Student Paper	1%
3	cris.vtt.fi Internet Source	<1%
4	Submitted to University of the Phillipines Student Paper	<1%
5	Nurul Zafirah Abd.Khalim Khafidz, Zahira Yaakob, Kean Long Lim, Sharifah Najiha Timmiati. "The kinetics of lightweight solid-state hydrogen storage materials: A review", International Journal of Hydrogen Energy, 2016 Publication	<1%

6	Internet Source	<1%
7	Z.H. Pan, C.Y. Zhao. "Gas–solid thermochemical heat storage reactors for high-temperature applications", Energy, 2017 Publication	<1%
8	C.G. Garay-Reyes, M.A. Ruiz-Esparza-Rodríguez, J.M. Mendoza-Duarte, I. Estrada Guel et al. "Effect of Fe impurities and pure Cr additions on microstructure of nanostructured WC-10Co alloy sintered by HIP", Journal of Alloys and Compounds, 2019 Publication	<1%
9	hdl.handle.net Internet Source	<1%
10	Gu, H.. "Hydrogen storage properties of Mg-Ni-Cu prepared by hydriding combustion synthesis and mechanical milling (HCS+MM)", International Journal of Hydrogen Energy, 200903 Publication	<1%
11	Jiguang Zhang, Yunfeng Zhu, Linglong Yao, Cheng Xu, Yana Liu, Liquan Li. "State of the art multi-strategy improvement of Mg-based hydrides for hydrogen storage", Journal of Alloys and Compounds, 2018 Publication	<1%

12	"Simple Metal and Intermetallic Hydrides", Fuel Cells and Hydrogen Energy, 2009 Publication	<1%
13	Jinzhe Lyu, Andrey Lider, Viktor Kudiiarov. "Using Ball Milling for Modification of the Hydrogenation/Dehydrogenation Process in Magnesium-Based Hydrogen Storage Materials: An Overview", Metals, 2019 Publication	<1%

Exclude quotes	Off	Exclude matches	Off
Exclude bibliography	On		